



# Fabrication of PVDF hierarchical fibrillar structures using electrospinning for dry-adhesive applications

Rahul Sahay<sup>1</sup>, Hashina Parveen<sup>1</sup>, Avinash Baji<sup>1,\*</sup>, V. Anand Ganesh<sup>1</sup>, and Anupama Sargur Ranganath<sup>1</sup>

<sup>1</sup>Division of Engineering Product Development, Singapore University of Technology and Design (SUTD), 8 Somapah Rd, Singapore 487372, Singapore

Received: 21 July 2016

Accepted: 25 October 2016

Published online:

4 November 2016

© Springer Science+Business Media New York 2016

## ABSTRACT

We report the fabrication of hierarchical poly(vinylidene fluoride) (PVDF) fibrous structures using a unique fabrication technique based on electrospinning. Electrospinning was used to fabricate aligned PVDF fibrous membranes. These membranes were then brought in contact with anodized aluminum oxide (AAO) template and then heat-treated above the glass transition temperature ( $T_g$ ) of the polymer to assist the flow of polymer within the cylindrical pores of AAO template. Scanning electron microscopy images confirmed that this approach lead to the growth of nanopillars on the surface of PVDF fibers. Nanoindenter was used to measure the pull-off force that was required to completely detach the indenter from the samples. To investigate the effect of hierarchy, pull-off force required to detach the indenter from neat PVDF fibers was determined and compared with the pull-off force recorded for hierarchical fibers. The effect of indentation depth was also investigated on both PVDF fibers and PVDF fiber with nanopillars. Significant pull-off force recorded indicates that these PVDF hierarchical fibrous structures can be potentially used for dry-adhesive applications.

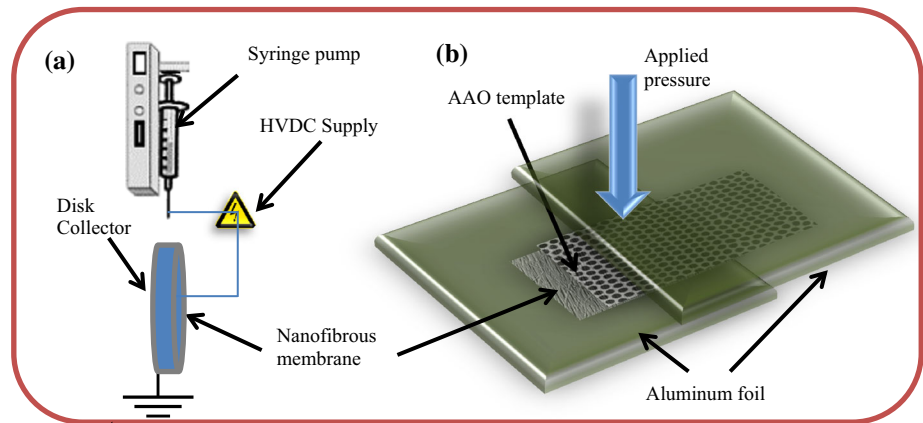
## Introduction

Climbing and adhering capabilities of geckos and certain insects have attracted huge amount of interest among researchers [1, 2]. The climbing and adhering abilities of these animals are ascribed to the hierarchical fibrillar structures found on their feet that interact with surfaces through van der Waals forces [3]. When millions of these fibrils come in contact with the surface, the numerous weak van der Waals forces add up and constitute an appreciable force for

the animal to adhere to the surface [4–7]. In an attempt to develop synthetic dry adhesives for wall-climbing robot applications, researchers focused their attention on mimicking the architecture and geometry of natural materials. For such applications, it is desirable that the synthetic structures should not only adhere to surfaces, but should also detach easily when they are peeled off at certain angles [8]. Additionally, the synthetic structures should maintain their adhesion strength over repeated attachment–detachment cycles [9].

Address correspondence to E-mail: avinash\_baji@sutd.edu.sg

**Figure 1** **a** Schematic of the electrospinning technique used to produce Sample A (neat PVDF fibers), and **b** schematic of the setup used to produce Sample B (hierarchical PVDF fibrous structures).



Several micro/nano-fabrication techniques such as nanoimprinting, micro/nanomolding, lithography, and chemical vapor deposition have been used to fabricate synthetic dry-adhesives [10–16]. However, most studies focused on fabricating fibrillar structures based on only micro- or nano-fibrils. These arrays of micro- or nano-fibrils only resemble the spatulas of the natural materials. Remarkable adhesion on smooth surfaces is reported with the use of polymer-based flat-tipped micropillars and carbon nanotube-based aligned arrays [16, 17]. However, when the roughness of the target surface is increased, the adhesion decreases as the polymer-based micropillars and carbon nanotube-based aligned arrays do not come in close contact with the surface [18, 19]. Adhesives based on hierarchical multiscale structures can address this issue as the hierarchical structures conform to wide variety of rough surfaces [18].

In this study, we aim to mimic the hierarchical design of natural materials using electrospinning combined with template wetting approach. Electrospinning is employed as it is an effective technique for fabricating high aspect-ratio polymeric fibers. These electrospun fibers being separate entities mimic the contact spitting nature of seta. The second level of the hierarchy is fabricated with the help of porous anodic aluminum oxide (AAO) template, which is frequently used to fabricate dense arrays of high aspect-ratio nanopillars [20, 21]. These high aspect-ratio nanopillars fabricated on electrospun fibers mimic spatulas of natural adhesive. This two-step processing technique enables us to control the dimensions of the structures at each level of hierarchy [22]. The dimension of the structures in the first level of the hierarchy is determined by the diameter

of the electrospun fibers, while the dimension of the structures in the second level of the hierarchy is determined by the pore size of the AAO template. We demonstrate that this fabrication technique is useful to grow nanopillars on the surface of the micron-sized fibers. Following this, we investigate the adhesion performance of these hierarchical structures and compare its adhesion behavior with that of neat fibers. Our results show that the hierarchical samples demonstrate improved adhesion behavior compared to neat fibers.

## Materials and methods

### Materials

Poly(vinylidene fluoride) (PVDF,  $M_w = 360,000$ ), *N,N*-dimethyl acetamide (DMAc), and acetone were procured from Sigma-Aldrich, Singapore. AAO templates with 250 nm pore diameter and 0.5 mm thickness were procured from Shanghai Shangmu Technology Co. Ltd., China.

### Fabrication

5.75 g of poly(vinylidene fluoride) was dissolved in 15 ml solvent mixture of DMAc and acetone in 1:2 (volume ratio). This solution was mechanically stirred at 50 °C for 12 h. The homogeneous solutions were then electrospun using an Invenso Nanospinner 24, Turkey to produce PVDF fibrous membrane. Electrospinning [23–26] was conducted at 1 kV/cm electric field and 1.5 ml/h flow rate. Relative humidity and the temperature were maintained at ~60% and ~25 °C, respectively. The solution was

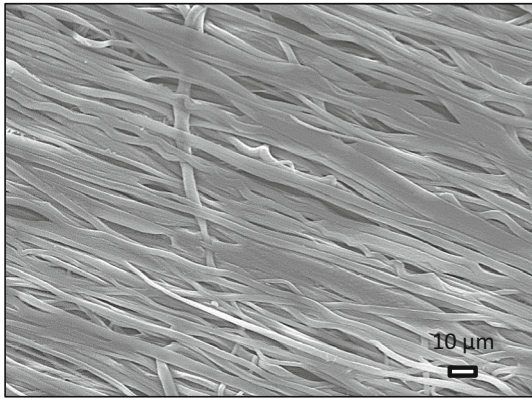


**Figure 2** SEM image of aligned PVDF fibers collected on a rotating disk collector.

emanating from a brass needle with 1 and 3 mm as inner and outer diameter, respectively. The electrospun fibers were then collected on a disk collector rotating at 3000 rpm (see Fig. 1a). These PVDF fibrous membranes were then heated at 80 °C for 24 h to evaporate any residual solvent. These neat PVDF fibrous samples are referred to as Sample A.

To prepare hierarchical fibrous samples, Sample A with  $1 \times 1 \text{ cm}^2$  cross-sectional area was brought in contact with AAO template of similar size as shown in Fig. 1b. The setup was then placed in a hydraulic press (model: 3912, Carver Inc., USA). The pressure was kept to  $\sim 40 \text{ kPa}$ , whereas temperature was varied from 40 to 80 °C and soaking time was varied from 5 to 20 min. Following this, samples were removed from the chamber and quenched in air. The PVDF membrane is then peeled-off from the AAO template to obtain ordered arrays of nanopillars on the surface of the PVDF fibers. These hierarchical PVDF fibrous samples are referred to as Sample B.

## Characterization

The morphology of Sample A and Sample B were studied using a field emission scanning electron microscope (SEM, JEOL, JSM-7600F).

Pull-off force of these samples was measured using a TI 950 triboindenter by Hysitron Inc., USA. The tests were performed with a 60° conical flat diamond indenter (diameter  $\sim 10 \mu\text{m}$ ). The indenter approached the sample with a constant loading rate of 10 nm/s, pressed against the samples to a predefined depth, and then withdrawn with a constant withdrawal rate of 500 nm/s. During retraction, the peak force required to completely detach the tip from the surface of the samples is documented as pull-off force. These measurements were conducted on samples having cross-sectional area as  $0.5 \text{ cm}^2$  and thickness as  $\sim 200 \mu\text{m}$ . These samples were secured onto a magnetic stub, which was then fixed onto the magnetic sample holder of the triboindenter. Typically, these samples consisted of aligned PVDF fibers with void spaces (see Figs. 2, 3). Therefore, an optical microscope attached to the triboindenter was used to visualize the samples and ensure that only the fibrous area of the sample was indented. Further, precautions were taken to keep the indentation depths below 1/10th of the thickness of samples to eliminate substrate effect [27]. The sample was then indented at a selected region with increasing indentation depth to investigate the effect of indentation depth on pull-off force. Ample time ( $\sim 1 \text{ h}$ ) was taken between successive measurements to allow the samples to ease back to their unstrained state. Subsequent test locations were chosen to be at least  $20 \mu\text{m}$  away from the previous test location.

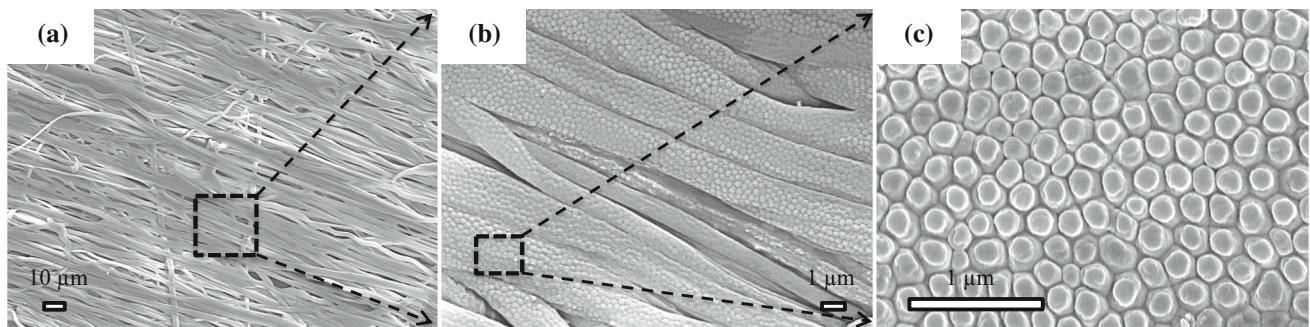


**Figure 3** a SEM image of PVDF hierarchical fibrous structures obtained via electrospinning combined with template wetting method. b and c high magnification SEM images of the PVDF hierarchical fibers.

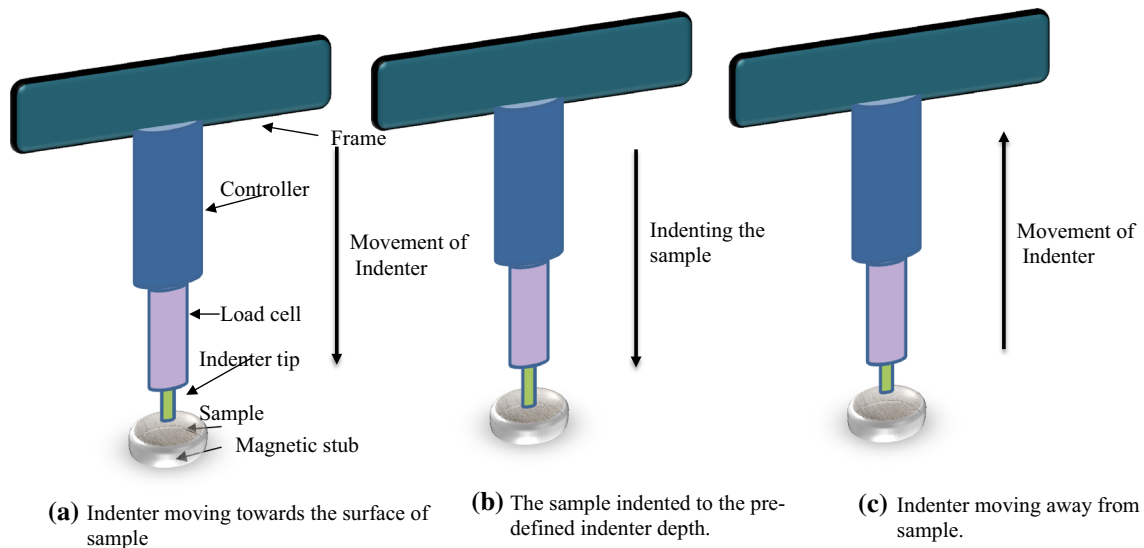


**Figure 4** Schematic illustrating the approach and retraction of the indenter over the sample.

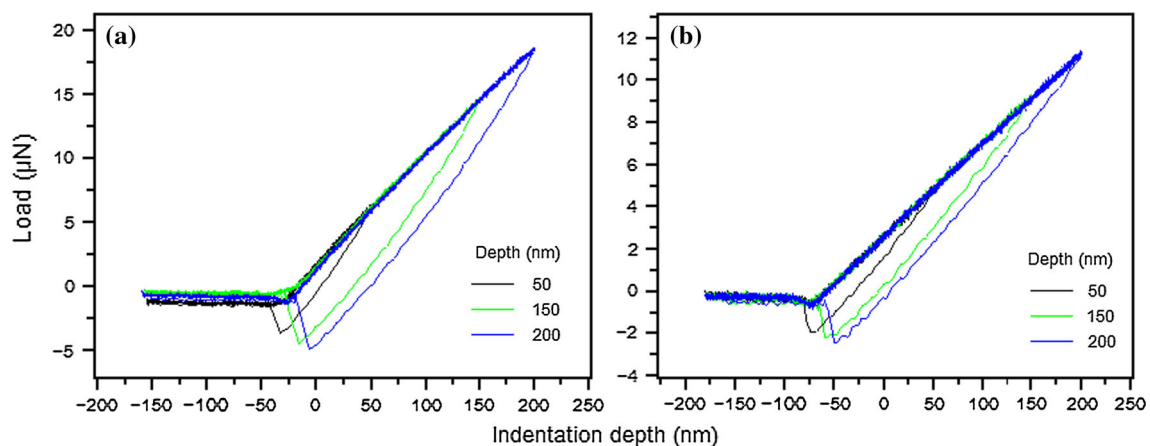


**Figure 5** Load versus indentation depth curves using nanoindenter for **a** hierarchical PVDF fibrous structures, and **b** neat PVDF fibrous membrane.

## Results and discussion

Figure 2 depicts SEM image of Sample A collected on a disk collector. Due to the presence of disk collector, electric field lines emanating from the metallic needle converges at the edge of the disk. Coupled with the high rotational speed (3000 rpm), aligned and closely packed PVDF fibers are obtained [28]. The average diameter of the PVDF fibers is estimated to be  $\sim 1.8 \mu\text{m}$ .

Hierarchical fibrous structures are fabricated by growing pillars on the surface of Sample A. This is achieved by bringing Sample A in contact with AAO template and heating the setup above the glass

transition temperature ( $T_g$ ) of the polymer. The temperature and time were varied from 40 to 80 °C and 5 to 20 min, respectively, to control the height of nanopillars [21, 29, 30]. Uniform distribution of nanopillars with an average height of  $\sim 200$  nm and an average diameter of  $\sim 250$  nm is obtained on the surface of PVDF fibers when the samples are heated at 50 °C for 10 min (see Fig. 3). These samples, known as Sample B, are investigated for their adhesion performance.

Subsequently, the adhesion performance of Sample A and Sample B is investigated using a nanoindenter [31, 32]. The measurements are performed by intending the samples with a pre-calibrated



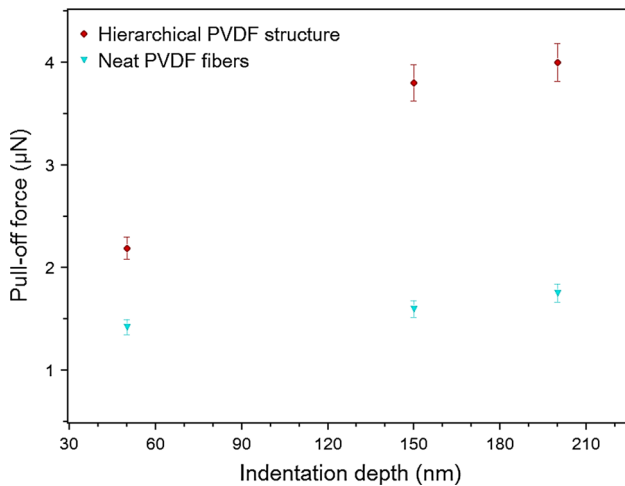


**Figure 6** Plot of pull-off force versus indentation depth recorded for Sample A and Sample B.

transducer attached to a flat circular diamond indenter actuated under displacement control. Initially, the indenter tip detects the surface of samples by approaching and touching it with a 1  $\mu\text{N}$  force. The indenter is then withdrawn to a height of 180 nm above the surface of samples to ensure that it is free of all surface forces. Then, the indenter approaches and indents the sample at a constant loading rate. Indentation depth is varied during measurements to investigate the effect of indentation depth on the measured pull-off force. The indenter is then withdrawn at a constant retraction rate (see Fig. 4). During the retraction of the indenter tip, it experiences van der Waals attractive forces. Therefore, the force required to completely separate the indenter tip from the surface of the sample is identified as the pull-off force.

Figures 5a, b show characteristic load-indentation depth curves recorded for Sample B and Sample A, respectively. The pull-off forces measured from Fig. 5a, b are then plotted as a function of indentation depth in Fig. 6. Figure 6 illustrates that pull-off force increases with an increase in the depth for both Sample A and Sample B. Figures 5 and 6 also reveal that pull-off forces recorded for Sample B are higher than those measured for Sample A, which is consistent with the results reported in the literature [33, 34]. The higher pull-off force recorded for Sample B is attributed to mechanics of the hierarchical sample and increased conformity of the sample to the surface of the indenter. This explains the increase in pull-off

force with indentation depth [35]. Complete analysis is beyond the scope of this study. The pull-off force for these samples increased from 2.19 to 4.0  $\mu\text{N}$  when the indentation depth is increased from 50 to 200 nm. The measured pull-off force recorded for Sample B is comparable with those measured for poly(dimethylsiloxane) (PDMS) and vertically oriented carbon nanotubes (VACNTs) [36].

The pull-off force is seen to reduce for Sample B when the depth of indentation is increased above 200 nm. However, the indentation depth had no influence on the measured pull-off force recorded for Sample A. The decrease in the pull-off force for Sample B is attributed to plastic deformation of the PVDF nanopillars due to excess applied load. For Sample A, pull-off force is seen to increase from 1.42 to 1.75  $\mu\text{N}$  with an increase in the depth from 50 to 200 nm. Typically, these stiff unstructured samples are unable to adapt to the irregularities present on the surface. Their poor conformity to the indenter surface is responsible for abysmal pull-off force recorded for Sample A. These results are in agreement with the Johnson–Kendall–Roberts (JKR) theory, which envisages that pull-off force for unstructured samples does not vary with indentation depth/preload [37].

## Conclusion

In conclusion, we fabricated PVDF hierarchical structure using electrospinning combined with a template wetting method for dry-adhesive applications. Pull-off force recorded for these hierarchical fibrous structures was investigated and compared with those of neat fibrous samples using a nanoindenter. Hierarchical fibrous samples exhibited higher pull-off force in comparison to neat fibrous samples. Higher pull-off force for PVDF hierarchical fibrous samples is attributed to an increase in conformity with the surface of indenter tip. These results demonstrate that these PVDF hierarchical fibrous structures can be potentially used for a wide variety of dry-adhesive applications.

## Acknowledgements

The authors would like to acknowledge the support of SUTD-MIT International Design Centre (Project No. IDG31400101). The authors also acknowledged the

financial support of SUTD start-up grant (Grant No: SRG-EPD-2013–055).

## References

- [1] Arzt E (2006) Biological and artificial attachment devices: lessons for materials scientists from flies and geckos. *Mater Sci Eng* 26:1245–1250
- [2] Meyers MA, Chen P-Y, Lin AY-M, Seki Y (2008) Biological materials: structure and mechanical properties. *Prog Mater Sci* 53:1–206
- [3] Autumn K, Sitti M, Liang YA, Peattie AM, Hansen WR, Sponberg S, Kenny TW, Fearing R, Israelachvili JN, Full RJ (2002) Evidence for van der waals adhesion in gecko setae. *Proc Natl Acad Sci USA* 99:12252–12256
- [4] Hansen W, Autumn K (2005) Evidence for self-cleaning in gecko setae. *Proc Natl Acad Sci USA* 102:385–389
- [5] Autumn K, Majidi C, Groff R, Dittmore A, Fearing R (2006) Effective elastic modulus of isolated gecko setal arrays. *J Exp Biol* 209:3558–3568
- [6] Autumn K, Hsieh S, Dudek D, Chen J, Chitaphan C, Full R (2006) Dynamics of geckos running vertically. *J Exp Biol* 209:260–272
- [7] Yao H, Gao H (2007) Mechanical principles of robust and releasable adhesion of gecko. *J Adhes Sci Technol* 21:1185–1212
- [8] Parness A, Soto D, Esparza N, Gravish N, Wilkinson M, Autumn K, Cutkosky M (2009) A microfabricated wedge-shaped adhesive array displaying gecko-like dynamic adhesion, directionality and long lifetime. *J R Soc Interface* 6:1223–1232
- [9] Sahay R, Low HY, Baji A, Foong S, Wood KL (2015) A state-of-the-art review and analysis on the design of dry adhesion materials for applications such as climbing micro-robots. *RSC Adv* 5:50821–50832
- [10] Autumn K (2006) Properties, principles, and parameters of the gecko adhesive system. In: Smith AM, Callow JA (eds) *Biological adhesives*. Springer, Heidelberg, pp 225–256
- [11] Afferrante L, Grimaldi G, Demelio G, Carbone G (2015) Direction-dependent adhesion of micro-walls based biomimetic adhesives. *Int J Adhes Adhes* 61:93–98
- [12] Sahay R, Baji A, Ranganath AS, Anand Ganesh V (2017) Durable adhesives based on electrospun poly(vinylidene fluoride) fibers. *J Appl Polym Sci* 134(44393):1–7
- [13] Greiner C, Arzt E, Del Campo A (2009) Hierarchical gecko-like adhesives. *Adv Mater* 21:479–482. doi:10.1002/adma.200801548
- [14] Gillies AG, Fearing RS (2011) Shear adhesion strength of thermoplastic gecko-inspired synthetic adhesive exceeds material limits. *Langmuir* 27:11278–11281. doi:10.1021/la202085j
- [15] Ge L, Sethi S, Ci L, Ajayan PM, Dhinojwala A (2007) Carbon nanotube-based synthetic gecko tapes. *Proc Natl Acad Sci USA* 104:10792–10795. doi:10.1073/pnas.0703505104
- [16] Del Campo A, Greiner C, Álvarez I, Arzt E (2007) Patterned surfaces with pillars with controlled 3D tip geometry mimicking bioattachment devices. *Adv Mater* 19:1973–1977
- [17] Ge L, Sethi S, Ci L, Ajayan PM, Dhinojwala A (2007) Carbon nanotube-based synthetic gecko tapes. *Proc Natl Acad Sci USA* 104:10792–10795
- [18] Murphy MP, Kim S, Sitti M (2009) Enhanced adhesion by gecko-inspired hierarchical fibrillar adhesives. *ACS Appl Mater Interfaces* 1:849–855
- [19] Aksak B, Murphy MP, Sitti M.: Gecko inspired micro-fibrillar adhesives for wall climbing robots on micro/nanoscale rough surfaces. *IEEE international conference on 2008 robotics and automation, ICRA 2008*. pp 3058–3063 2008
- [20] Mijangos C, Hernández R, Martín J (2016) A review on the progress of polymer nanostructures with modulated morphologies and properties, using nanoporous AAO templates. *Prog Polym Sci* 54:148–182. doi:10.1016/j.progpolymsci.2015.10.003
- [21] Martin J, Maiz J, Sacristan J, Mijangos C (2012) Tailored polymer-based nanorods and nanotubes by “template synthesis”: from preparation to applications. *Polymer* 53:1149–1166
- [22] Sahay R, Parveen H, Ranganath AS, Ganesh VA, Baji A (2016) On the adhesion of hierarchical electrospun fibrous structures and prediction of their pull-off strength. *RSC Adv* 6:47883–47889
- [23] Sahay R, Teo C, Chew Y (2013) New correlation formulae for the straight section of the electrospun jet from a polymer drop. *J Fluid Mech* 735:150–175
- [24] Reneker DH, Yarin AL, Fong H, Koombhongse S (2000) Bending instability of electrically charged liquid jets of polymer solutions in electrospinning. *J Appl Phys* 87:4531–4547
- [25] Yarin AL, Kataphinan W, Reneker DH (2005) Branching in electrospinning of nanofibers. *J Appl Phys* 98:1–12
- [26] Yarin AL, Koombhongse S, Reneker DH (2001) Taylor cone and jetting from liquid droplets in electrospinning of nanofibers. *J Appl Phys* 90:4836–4846
- [27] Wang M, Liechti KM, White JM, Winter RM (2004) Nanoindentation of polymeric thin films with an interfacial force microscope. *J Mech Phys Solids* 52:2329–2354
- [28] Sahay R, Thavasi V, Ramakrishna S (2011) Design modifications in electrospinning setup for advanced applications. *J Nanomater* 2011:1–18

- [29] Chen J-T, Chen W-L, Fan P-W (2011) Hierarchical structures by wetting porous templates with electrospun polymer fibers. *ACS Macro Lett* 1:41–46
- [30] Cao G, Liu D (2008) Template-based synthesis of nanorod, nanowire, and nanotube arrays. *Adv Coll Interface Sci* 136:45–64
- [31] Northen MT, Turner KL (2005) A batch fabricated biomimetic dry adhesive. *Nanotechnology* 16:1159–1166
- [32] Schaber CF, Heinlein T, Keeley G, Schneider JJ, Gorb SN (2015) Tribological properties of vertically aligned carbon nanotube arrays. *Carbon* 94:396–404. doi:[10.1016/j.carbon.2015.07.007](https://doi.org/10.1016/j.carbon.2015.07.007)
- [33] Gorb S, Varenberg M, Peressadko A, Tuma J (2007) Biomimetic mushroom-shaped fibrillar adhesive microstructure. *J R Soc Interface* 4:271–275
- [34] Peressadko A, Gorb SN (2004) When less is more: experimental evidence for tenacity enhancement by division of contact area. *J Adhes* 80:247–261
- [35] Greiner C, del Campo A, Arzt E (2007) Adhesion of bioinspired micropatterned surfaces: effects of pillar radius, aspect ratio, and preload. *Langmuir* 23:3495–3502
- [36] Chen B, Goldberg Oppenheimer P, Shean TA, Wirth CT, Hofmann S, Robertson J (2012) Adhesive properties of gecko-inspired mimetic via micropatterned carbon nanotube forests. *J Phys Chem C* 116:20047–20053
- [37] Johnson K, Kendall K, Roberts A (1971) Surface energy and the contact of elastic solids. *Proc R Soc Lond A* 324:301–313